

Study of kinetic freeze-out parameters as function of rapidity in pp collisions at CERN SPS energies

Muhammad Waqas^{1,*}, H. M. Chen¹, Guang Xiong Peng^{1,†},
Abd Al Karim Haj Ismail^{2,3,‡}, Muhammad Ajaz⁴, Zafar wazir⁵, Ramoona Shehzadi⁶, Sabiha Jamal⁴, Atef AbdelKader^{2,3}

¹*School of Nuclear Science and Technology, University of Chinese Academy of Sciences, Beijing 100049, Peoples Republic of China,*

²*Department of Mathematics and Science, Ajman University, PO Box 346, UAE,*

³*Nonlinear Dynamics Research Center (NDRC), Ajman University, PO Box 346, UAE,*

⁴*Department of Physics, Abdul Wali Khan University Mardan, 23200 Mardan, Pakistan,*

⁵*Department of physics, Ghazi University, Dera Ghazi Khan, Pakistan,*

⁶*Department of Physics, University of the Punjab, Lahore, Pakistan*

Abstract: We used the blast wave model with Boltzmann Gibbs statistics and analyzed the experimental data measured by NA61/SHINE Collaboration in inelastic (INEL) proton-proton collisions at different rapidity slices at different center-of-mass energies. The particles used in this study are π^+ , π^- , K^+ , K^- and \bar{p} . We extracted kinetic freeze-out temperature, transverse flow velocity and kinetic freeze-out volume from the transverse momentum spectra of the particles. We observed that the kinetic freeze-out temperature is rapidity and energy dependent, while transverse flow velocity does not depend on them. Furthermore, we observed that the kinetic freeze-out volume is energy dependent but it remains constant with changing the rapidity. We also observed that all these three parameters are mass dependent. In addition, with the increase of mass, the kinetic freeze-out temperature increases, and the transverse flow velocity as well as kinetic freeze-out volume decreases.

Keywords: rapidity, transverse momentum spectra, kinetic freeze-out temperature, transverse flow velocity, kinetic freeze-out volume.

PACS: 25.75.Ag, 25.75.Dw, 24.10.Pa

1 Introduction

To study the dynamics of high energy collisions, the transverse momentum spectra of the particles are the most important tool to be used. The proton-proton (pp) interactions are used as the baseline and are significant for understanding the particle production mechanism [1].

In order to understand the nuclear reaction mechanism and evolution characteristic, the excitation functions of some physical quantities (i.e different temperatures including initial temperature (T_i), effective temperature (T), chemical freeze-out temperature (T_{ch}) and kinetic freeze-out temperature (T_0) and mean transverse momentum $\langle p_T \rangle$) are very important. We can learn more about the high energy collision process by analyzing the excitation functions of T_0 , $\langle p_T \rangle$, T_i , transverse

flow velocity (β_T) and kinetic freeze-out volume (V), in which the excitation functions of the above parameters can be extracted from the transverse momentum spectra (p_T) of the particles. The parameters mentioned above are discussed in detail in Ref. [2–7]. However, we would like to further discuss the temperature here, because temperature is one of the most significant concepts in thermodynamics and statistical mechanics [8], and it describes the excitation degree of the interacting system in sub-atomic physics.

There are different kinds of temperature discussed in the literature [3–7], which corresponds to different collision stages and it is expected that they vary at different stages due to the system evolution. In the present work, we will study the final state particles, therefore we are interested in kinetic freeze-out temperature which occurs at the stage of kinetic freeze-out. In literature,

*E-mail: waqas_phy313@yahoo.com

†Correspondence: gxpeng@ucas.ac.cn

‡Correspondence: a.hajismail@ajman.ac.ae

there are various kinetic freeze-out scenarios including single, double, triple and multiple kinetic freeze-out scenarios [9–14]. In addition, there are various claims and dependencies of kinetic freeze-out temperature on centrality [5–10, 13, 15–17] and collision energy [2, 3, 10, 18]. In our recent work, it is observed that the kinetic freeze-out temperature also depends on coalescence and isospin symmetry [19]. We wonder if T_0 is also expected to depend on rapidity. For this purpose, we analyze the final state identified particles in different rapidity slices at different energies in pp collisions and extracted the kinetic freeze-out temperature, transverse flow velocity (β_T) and kinetic freeze-out volume from the transverse momentum spectra of the particles by using blast wave model with Boltzmann Gibbs statistics [20, 21].

The structure of β_T and V is very complex and they are studied in various publications. For centrality dependence, most of the studies agree that β_T and V decrease with decreasing centrality [4,6,7,13,18], but the dependence of β_T on collision energy is a matter of contradiction [10, 17, 18].

The remainder of the paper includes formalism and method, results and discussions, and conclusions.

2 The model and method

It is experimentally established that the system which is produced during high energy collision has an azimuthal anisotropy due to the difference in flow velocities along various directions. This azimuthal anisotropy occurs due to some initial state geometric effects that rise during the collision process. Therefore, it can be testified that the departing particles must carry some impressions of such effects that can have an impact on the nature of the spectra. In order to include such effects, various models are suggested [22–32]. In the present work we used the blast wave model with Boltzmann Gibbs statistics (BGBW) [20,21]. Blast wave model is a hydrodynamical based model. It includes the random thermal motion as well as the flow properties of the particles. Including the azimuthal anisotropy, the blast wave model gives a complete picture of the quark gluon plasma (QGP) evolution dynamics. The transverse momentum spectrum of BGBW is given as

$$f(p_T) = \frac{1}{N} \frac{dN}{dp_T} = \frac{1}{N} \frac{gV}{(2\pi)^2} p_T m_T \int_0^R r dr \times I_0 \left[\frac{p_T \sinh(\rho)}{T} \right] K_1 \left[\frac{m_T \cosh(\rho)}{T} \right], \quad (1)$$

where N represents the number of particles, g is the spin degeneracy factor of the particle which is different for different particles (based on $g_n = 2S_n + 1$, while S_n is

the spin of the particle), V denotes the volume of the system under consideration, m_T ($m_T = \sqrt{p_T^2 + m_0^2}$) is the transverse mass, I_0 and K_1 are the modified Bessel functions, $\rho = \tanh^{-1}[\beta(r)]$, $\beta(r) = \beta_S(r/R)^{n_0}$ is the transverse radial flow of the thermal source at radius $0 \leq r \leq R$ with surface velocity β_S . We used $n_0 = 2$ to be compatible with ref. [20] in the present work, which it closely resembles hydrodynamic profile as mentioned in ref. [20], and results in $\beta_T = 0.5\beta(S)$. Because the maximum value of $\beta(S)$ is $1c$, the maximum value of β_T is $0.5c$. If $n_0 = 1$, it results in $\beta_T = (2/3)\beta(S)$. Therefore, the maximum β_T is $(2/3)c$. If n_0 is used to be a non-integer from that less than 1 to above 2, then it corresponds to the centrality from center to periphery. This can lead to a large fluctuation in β_T . The value of $n_0 = 1$ or 2 does not effect the result because it is not very sensitive, but if it is taken as a free parameter, then it leads to a large fluctuation in β_T , and naturally a small change in T_0 occurs. In general, $\beta_T = (2/R^2) \int_0^R r \beta(r) dr = 2\beta_S / (n_0 + 2) = 2\beta_S / 3$.

We can use Eq. (1) for the fitting of p_T spectra and extract the parameters T_0 , β_T and V . Eq.(1) is applicable in only soft p_T ($p_T = 2-3$ GeV/c) regime of the p_T spectra and is valid for a narrow p_T range. In the range of $p_T > 3$ GeV/c, a hard scattering process should be brought into consideration, which is studied in our previous studies [5, 8, 9, 13, 16, 18].

3 Results and discussion

The transverse momentum (p_T) spectra of π^+ and π^- produced in inelastic (INEL) proton-proton (pp) collisions [33] at different rapidity slices at different energies are represented in fig. 1 and fig. 2, respectively. The symbols represent the experimental data of NA61/SHINE Collaboration at CERN (European Council for Nuclear Research) and different symbols represents the p_T spectra of the particles at different rapidity slices. The collision energy and rapidity slices are labeled in each panel. The solid curves on the experimental data are our fitting by using Eq. (1). Different panels corresponds to different collision energies. The lower layer in each panel represents the corresponding ratio of data/fit. The related values of free parameters, and χ^2 and degrees of freedom (dof) are presented in table 1. One can see that Eq. (1) provides an approximately well fitting of the data at all rapidity slices.

Fig 3. and fig. 4 are similar to fig. 1 and 2, but they show the transverse momentum spectra of K^+ and K^- respectively at different rapidity slices in pp collisions at different energies. The symbols represent the experimental data of NA61/SHINE Collaboration [33]

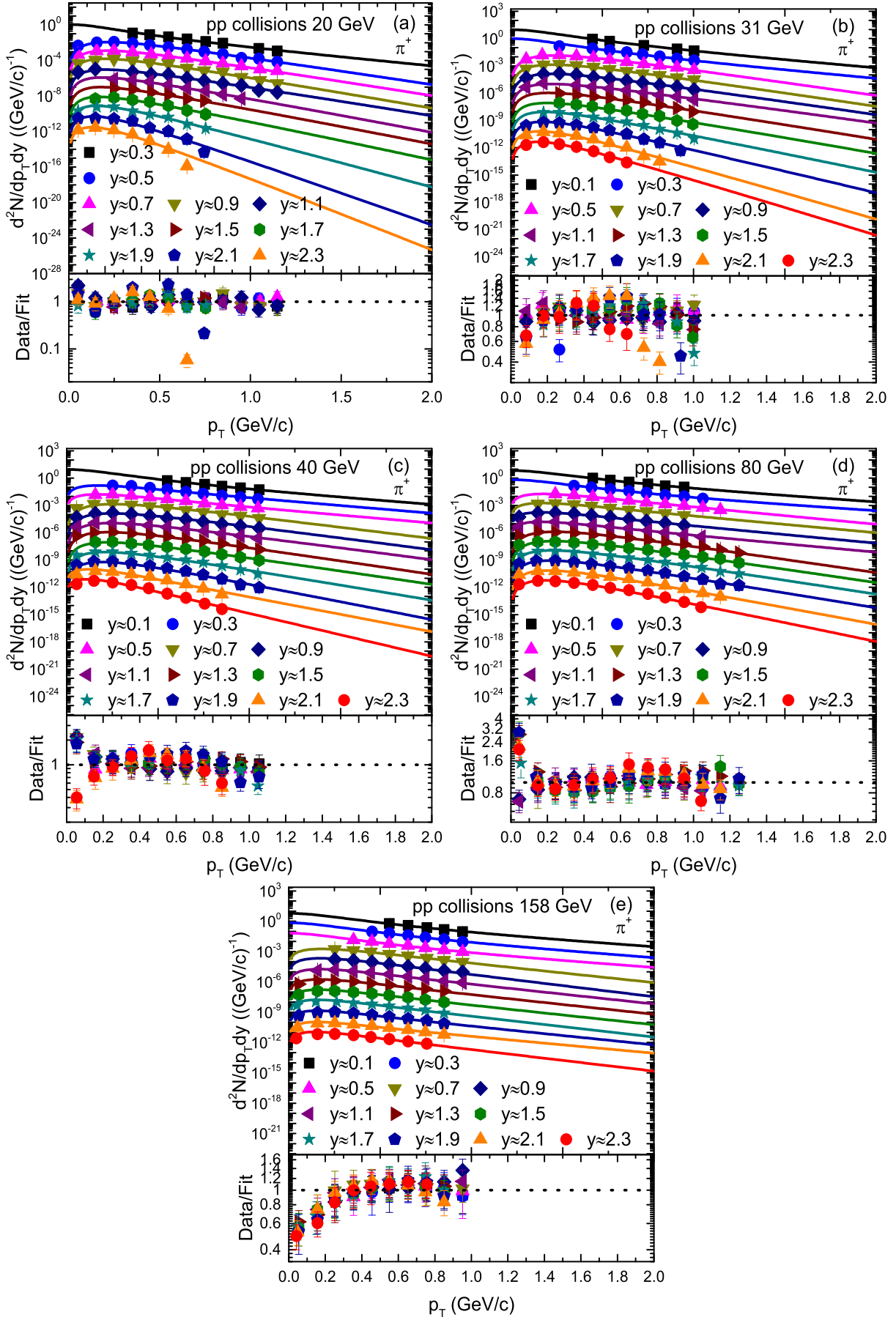


Fig. 1. Transverse momentum spectra of π^+ produced in different rapidity slices in pp collisions. Panel (a)-(e) corresponds to 20, 31, 40, 80 and 158 GeV energy respectively. The symbols represent the experimental data of NA61/SHINE Collaboration measured at CERN [33]. The curves are the results of our fits by the Blast Wave

Table 1. Values of free parameters (T_0 and β_T), normalization constant (N_0), χ^2 , and degree of freedom (dof) corresponding to the curves in Figs. 1-6.

Collisions	Rapidity	Particle	T_0 (GeV)	β_T (c)	$V(fm^3)$	N_0	χ^2/dof
Fig. 1 p-p 20 GeV	y=0.3	π^+	0.076 ± 0.005	0.410 ± 0.010	1000 ± 100	$9.5E - 7 \pm 5E - 8$	5/4
	y=0.5	-	0.070 ± 0.004	0.280 ± 0.007	1000 ± 108	$5.0E - 7 \pm 4E - 8$	4/8
	y=0.7	-	0.066 ± 0.005	0.284 ± 0.010	900 ± 90	$6E - 8 \pm 6E - 9$	3.5/8
	y=0.9	-	0.061 ± 0.006	0.284 ± 0.011	920 ± 120	$7E - 9 \pm 6E - 10$	9/8
	y=1.1	-	0.056 ± 0.004	0.328 ± 0.008	900 ± 105	$4.5E - 10 \pm 4E - 11$	11/7
	y=1.3	-	0.051 ± 0.004	0.312 ± 0.012	800 ± 90	$6.4E - 11 \pm 5E - 12$	4/4
	y=1.5	-	0.048 ± 0.006	0.320 ± 0.010	860 ± 85	$4.9E - 12 \pm 5E - 13$	1/2
	y=1.7	-	0.045 ± 0.004	0.313 ± 0.007	870 ± 80	$3.8E - 13 \pm 4E - 14$	9/3
	y=1.9	-	0.041 ± 0.005	0.270 ± 0.011	800 ± 70	$4E - 14 \pm 6E - 15$	5/4
	y=2.1	-	0.038 ± 0.004	0.200 ± 0.013	810 ± 200	$2.5E - 15 \pm 4E - 16$	118/4
y=2.3	-	0.034 ± 0.005	0.200 ± 0.008	800 ± 150	$1.5E - 16 \pm 7E - 17$	120/3	
Fig. 2 p-p 20 GeV	y=0.3	π^-	0.079 ± 0.006	0.421 ± 0.013	1000 ± 100	$6.5E - 7 \pm 6E - 8$	3/3
	y=0.5	-	0.070 ± 0.005	0.280 ± 0.008	1000 ± 98	$3.5E - 7 \pm 5E - 8$	6/5
	y=0.7	-	0.067 ± 0.006	0.282 ± 0.011	920 ± 70	$4E - 8 \pm 4E - 9$	3/6
	y=0.9	-	0.061 ± 0.004	0.278 ± 0.009	920 ± 110	$4.5E - 9 \pm 6E - 10$	7/4
	y=1.1	-	0.059 ± 0.005	0.334 ± 0.011	900 ± 115	$7.2E - 11 \pm 7E - 12$	8/2
	y=1.3	-	0.053 ± 0.006	0.323 ± 0.010	830 ± 69	$3.6E - 11 \pm 4E - 12$	3/0
	y=1.5	-	0.050 ± 0.005	0.319 ± 0.012	854 ± 93	$2.2E - 12 \pm 6E - 13$	0.2/-
	y=1.7	-	0.047 ± 0.006	0.319 ± 0.009	857 ± 75	$1.5E - 13 \pm 5E - 14$	1/-
	y=1.9	-	0.043 ± 0.005	0.276 ± 0.010	808 ± 75	$1.5E - 14 \pm 5E - 15$	1/-
	y=2.1	-	0.040 ± 0.006	0.210 ± 0.011	819 ± 80	$1E - 15 \pm 5E - 16$	10/-
y=2.3	-	0.034 ± 0.004	0.200 ± 0.008	800 ± 110	$6E - 17 \pm 7E - 18$	1/-	
Fig. 1 p-p 31 GeV	y=0.1	π^+	0.088 ± 0.006	0.410 ± 0.011	1400 ± 114	$7E - 6 \pm 4E - 7$	0.1/1
	y=0.3	-	0.083 ± 0.005	0.410 ± 0.009	1200 ± 210	$7.9E - 7 \pm 5E - 8$	21/4
	y=0.5	-	0.078 ± 0.004	0.256 ± 0.008	1400 ± 100	$4.2E - 7 \pm 3E - 8$	1.5/7
	y=0.7	-	0.075 ± 0.005	0.268 ± 0.012	1200 ± 108	$4.8E - 8 \pm 4E - 9$	2/7
	y=0.9	-	0.071 ± 0.004	0.293 ± 0.009	1300 ± 90	$4.8E - 9 \pm 4E - 10$	2/7
	y=1.1	-	0.067 ± 0.006	0.303 ± 0.011	1230 ± 100	$4.2E - 10 \pm 5E - 11$	2/6
	y=1.3	-	0.063 ± 0.005	0.297 ± 0.010	1020 ± 110	$4.5E - 11 \pm 4E - 12$	3.5/5
	y=1.5	-	0.060 ± 0.005	0.279 ± 0.008	1140 ± 105	$3.1E - 12 \pm 4E - 13$	8/5
	y=1.7	-	0.056 ± 0.005	0.260 ± 0.009	1000 ± 70	$3.6E - 13 \pm 4E - 14$	31/6
	y=1.9	-	0.052 ± 0.004	0.233 ± 0.012	1070 ± 83	$2.7E - 14 \pm 4E - 15$	25/6
y=2.1	-	0.048 ± 0.004	0.190 ± 0.010	978 ± 76	$2.6E - 15 \pm 5E - 16$	80/5	
y=2.3	-	0.044 ± 0.005	0.204 ± 0.007	1000 ± 104	$1.8E - 16 \pm 4E - 17$	10/3	
Fig. 2 p-p 31 GeV	y=0.1	π^-	0.090 ± 0.005	0.425 ± 0.010	1420 ± 104	$5.5E - 6 \pm 6E - 7$	0.2/-
	y=0.3	-	0.086 ± 0.006	0.436 ± 0.011	1250 ± 110	$5.9E - 7 \pm 4E - 8$	16/-
	y=0.5	-	0.082 ± 0.006	0.253 ± 0.012	1423 ± 109	$3.4E - 7 \pm 5E - 8$	8/5
	y=0.7	-	0.078 ± 0.006	0.263 ± 0.008	1216 ± 128	$3.8E - 8 \pm 7E - 9$	11/5
	y=0.9	-	0.073 ± 0.006	0.286 ± 0.012	1310 ± 80	$3E - 9 \pm 5E - 10$	10/4
	y=1.1	-	0.069 ± 0.005	0.324 ± 0.012	1255 ± 90	$7E - 11 \pm 7E - 12$	2/3
	y=1.3	-	0.067 ± 0.006	0.288 ± 0.009	1057 ± 100	$2.5E - 11 \pm 5E - 12$	0.3/1
	y=1.5	-	0.063 ± 0.006	0.286 ± 0.009	1166 ± 112	$2E - 12 \pm 6E - 13$	3.5/1
	y=1.7	-	0.058 ± 0.006	0.270 ± 0.012	1040 ± 80	$2E - 13 \pm 4E - 14$	6/1
	y=1.9	-	0.057 ± 0.006	0.229 ± 0.009	1070 ± 92	$1.4E - 14 \pm 4E - 15$	6/1
y=2.1	-	0.050 ± 0.005	0.190 ± 0.008	1000 ± 93	$1.2E - 15 \pm 4E - 16$	10/1	
y=2.3	-	0.044 ± 0.005	0.199 ± 0.007	1040 ± 104	$9.4E - 17 \pm 4E - 18$	9/-	
Fig. 1 p-p 40 GeV	y=0.1	π^+	0.097 ± 0.005	0.415 ± 0.010	1700 ± 100	$6.7E - 6 \pm 5E - 7$	0.1/2
	y=0.3	-	0.093 ± 0.005	0.385 ± 0.007	1700 ± 103	$1E - 7 \pm 4E - 8$	3/5
	y=0.5	-	0.090 ± 0.005	0.385 ± 0.009	1600 ± 106	$1.1E - 7 \pm 4E - 8$	3.5/6
	y=0.7	-	0.086 ± 0.006	0.275 ± 0.011	1575 ± 100	$3.8E - 8 \pm 5E - 9$	14/7
	y=0.9	-	0.082 ± 0.006	0.276 ± 0.008	1540 ± 110	$3.7E - 9 \pm 4E - 10$	10/7
	y=1.1	-	0.078 ± 0.004	0.292 ± 0.010	1633 ± 100	$3.4E - 10 \pm 4E - 11$	6/7
	y=1.3	-	0.074 ± 0.005	0.269 ± 0.012	1400 ± 90	$3.5E - 11 \pm 4E - 12$	4/7
	y=1.5	-	0.070 ± 0.004	0.290 ± 0.010	1437 ± 96	$2.6E - 12 \pm 4E - 13$	3/6
	y=1.7	-	0.067 ± 0.004	0.265 ± 0.007	1500 ± 67	$2.1E - 13 \pm 5E - 14$	21/7
	y=1.9	-	0.063 ± 0.006	0.230 ± 0.008	1394 ± 100	$1.8E - 14 \pm 4E - 15$	20/7
y=2.1	-	0.059 ± 0.005	0.285 ± 0.012	1400 ± 70	$4.5E - 15 \pm 5E - 16$	58/5	
y=2.3	-	0.055 ± 0.006	0.235 ± 0.008	1400 ± 80	$3.2E - 16 \pm 5E - 17$	41/5	
Fig. 2 p-p 40 GeV	y=0.1	π^-	0.098 ± 0.006	0.418 ± 0.010	1700 ± 100	$4.6E - 6 \pm 4E - 7$	0.6/-
	y=0.3	-	0.095 ± 0.006	0.385 ± 0.009	1720 ± 105	$8E - 7 \pm 6E - 8$	1/3
	y=0.5	-	0.091 ± 0.005	0.384 ± 0.009	1611 ± 100	$7.6E - 8 \pm 7E - 9$	2/4
	y=0.7	-	0.087 ± 0.004	0.269 ± 0.012	1584 ± 110	$2.5E - 8 \pm 6E - 9$	7/5
	y=0.9	-	0.084 ± 0.005	0.270 ± 0.008	1500 ± 100	$2.6E - 9 \pm 5E - 10$	7/5
	y=1.1	-	0.080 ± 0.005	0.285 ± 0.009	1603 ± 90	$2.1E - 10 \pm 6E - 11$	14/4
y=1.3	-	0.076 ± 0.006	0.259 ± 0.010	1380 ± 85	$2.4E - 11 \pm 5E - 12$	10/3	

Table 1. Continue.

Collisions	Rapidity	Particle	T_0 (GeV)	β_T (c)	$V(fm^3)$	N_0	χ^2/dof
Fig. 1 p-p 80 GeV	y=1.5	-	0.072 ± 0.005	0.287 ± 0.011	1415 ± 73	$1.6E - 12 \pm 6E - 13$	4/2
	y=1.7	-	0.069 ± 0.006	0.265 ± 0.009	1490 ± 71	$1.6E - 13 \pm 5E - 14$	17/2
	y=1.9	-	0.064 ± 0.005	0.228 ± 0.010	1381 ± 87	$1.3E - 14 \pm 7E - 15$	14/2
	y=2.1	-	0.061 ± 0.004	0.292 ± 0.008	1380 ± 76	$2E - 16 \pm 5E - 17$	12/1
	y=2.3	-	0.057 ± 0.005	0.235 ± 0.013	1370 ± 78	$1.3E - 17 \pm 5E - 18$	73/-
	y=0.1	π^+	0.108 ± 0.006	0.425 ± 0.011	2000 ± 100	$4.9E - 6 \pm 4E - 7$	0.2/2
	y=0.3	-	0.104 ± 0.004	0.435 ± 0.008	1824 ± 70	$5.2E - 7 \pm 5E - 8$	1/4
	y=0.5	-	0.100 ± 0.005	0.342 ± 0.010	1800 ± 66	$1.1E - 7 \pm 3E - 8$	1/6
	y=0.7	-	0.095 ± 0.004	0.363 ± 0.010	1829 ± 100	$1.1E - 8 \pm 7E - 9$	0.4/5
	y=0.9	-	0.091 ± 0.005	0.364 ± 0.009	1892 ± 110	$9.5E - 10 \pm 6E - 11$	5/6
Fig. 2 p-p 80 GeV	y=1.1	-	0.087 ± 0.006	0.379 ± 0.012	1850 ± 103	$8.8E - 11 \pm 7E - 12$	7/7
	y=1.3	-	0.082 ± 0.005	0.239 ± 0.009	1790 ± 108	$3E - 11 \pm 6E - 12$	14/9
	y=1.5	-	0.078 ± 0.006	0.259 ± 0.008	1700 ± 160	$3E - 12 \pm 7E - 13$	11/9
	y=1.7	-	0.074 ± 0.005	0.258 ± 0.009	1766 ± 70	$2.7E - 13 \pm 6E - 14$	6/9
	y=1.9	-	0.070 ± 0.005	0.255 ± 0.011	1800 ± 103	$2E - 14 \pm 5E - 15$	15/9
	y=2.1	-	0.067 ± 0.004	0.228 ± 0.010	1710 ± 100	$1.7E - 15 \pm 5E - 15$	13/8
	y=2.3	-	0.062 ± 0.005	0.215 ± 0.011	1730 ± 97	$1.4E - 16 \pm 7E - 17$	17/7
	y=0.1	π^-	0.108 ± 0.006	0.437 ± 0.008	2000 ± 104	$4.4E - 6 \pm 6E - 7$	1/-
	y=0.3	-	0.106 ± 0.005	0.457 ± 0.009	1800 ± 100	$4.5E - 7 \pm 5E - 8$	1/2
	y=0.5	-	0.102 ± 0.006	0.349 ± 0.012	1780 ± 72	$9E - 8 \pm 5E - 9$	1/2
Fig. 1 p-p 158 GeV	y=0.7	-	0.097 ± 0.006	0.368 ± 0.012	1800 ± 110	$8.5E - 9 \pm 7E - 10$	1/3
	y=0.9	-	0.093 ± 0.006	0.367 ± 0.010	1820 ± 90	$7.3E - 10 \pm 4E - 11$	4/4
	y=1.1	-	0.088 ± 0.004	0.389 ± 0.011	1820 ± 108	$6.3E - 11 \pm 6E - 12$	4/4
	y=1.3	-	0.084 ± 0.004	0.235 ± 0.008	1760 ± 100	$2.2E - 11 \pm 6E - 12$	17/6
	y=1.5	-	0.080 ± 0.005	0.249 ± 0.009	1680 ± 100	$2E - 12 \pm 5E - 13$	16/4
	y=1.7	-	0.076 ± 0.006	0.260 ± 0.010	1735 ± 90	$1.4E - 13 \pm 4E - 14$	16/3
	y=1.9	-	0.072 ± 0.006	0.250 ± 0.008	1750 ± 86	$1.1E - 14 \pm 6E - 15$	9/2
	y=2.1	-	0.069 ± 0.005	0.220 ± 0.009	1680 ± 80	$1E - 15 \pm 5E - 15$	14/2
	y=2.3	-	0.064 ± 0.005	0.211 ± 0.012	1700 ± 70	$7E - 17 \pm 5E - 18$	15/-
	y=0.1	π^+	0.115 ± 0.004	0.425 ± 0.008	2250 ± 100	$4.2E - 6 \pm 5E - 7$	0.3/1
Fig. 2 p-p 158 GeV	y=0.3	-	0.111 ± 0.004	0.420 ± 0.009	2150 ± 70	$4.7E - 7 \pm 6E - 8$	0.4/2
	y=0.5	-	0.108 ± 0.004	0.430 ± 0.012	2160 ± 96	$4.4E - 8 \pm 5E - 9$	1/3
	y=0.7	-	0.104 ± 0.005	0.330 ± 0.011	2160 ± 60	$9.2E - 9 \pm 4E - 10$	0.5/4
	y=0.9	-	0.100 ± 0.006	0.300 ± 0.012	2200 ± 110	$1E - 9 \pm 6E - 10$	4/4
	y=1.1	-	0.095 ± 0.005	0.348 ± 0.010	2000 ± 106	$9.5E - 11 \pm 7E - 12$	5/5
	y=1.3	-	0.091 ± 0.004	0.360 ± 0.010	2000 ± 122	$9E - 12 \pm 6E - 13$	16/5
	y=1.5	-	0.087 ± 0.005	0.370 ± 0.011	1900 ± 120	$9E - 13 \pm 7E - 14$	13/5
	y=1.7	-	0.082 ± 0.006	0.370 ± 0.008	1900 ± 108	$8.6E - 14 \pm 6E - 15$	21/5
	y=1.9	-	0.078 ± 0.004	0.280 ± 0.012	1900 ± 107	$7.3E - 15 \pm 5E - 16$	19/5
	y=2.1	-	0.075 ± 0.006	0.423 ± 0.007	1990 ± 120	$5.5E - 16 \pm 5E - 17$	26/5
Fig. 3 p-p 20 GeV	y=2.3	-	0.070 ± 0.005	0.393 ± 0.008	2019 ± 110	$5E - 17 \pm 7E - 18$	42/4
	y=0.1	π^-	0.114 ± 0.004	0.440 ± 0.010	2235 ± 110	$3.9E - 6 \pm 7E - 7$	0.4/1
	y=0.3	-	0.112 ± 0.006	0.435 ± 0.012	2100 ± 80	$4.4E - 7 \pm 7E - 8$	0.1/2
	y=0.5	-	0.108 ± 0.004	0.430 ± 0.012	2160 ± 96	$4E - 8 \pm 5E - 9$	1.5/3
	y=0.7	-	0.105 ± 0.006	0.330 ± 0.010	2160 ± 90	$8.4E - 9 \pm 4E - 10$	1/4
	y=0.9	-	0.100 ± 0.006	0.330 ± 0.012	2200 ± 100	$8E - 10 \pm 5E - 11$	1/7
	y=1.1	-	0.096 ± 0.005	0.352 ± 0.011	2010 ± 91	$7E - 11 \pm 4E - 12$	2/7
	y=1.3	-	0.092 ± 0.005	0.366 ± 0.010	2120 ± 102	$6.4E - 12 \pm 4E - 13$	3/6
	y=1.5	-	0.087 ± 0.006	0.370 ± 0.010	1900 ± 100	$6E - 13 \pm 5E - 15$	3.5/7
	y=1.7	-	0.083 ± 0.005	0.370 ± 0.012	1909 ± 98	$5.6E - 14 \pm 5E - 15$	5/6
Fig. 3 p-p 20 GeV	y=1.9	-	0.080 ± 0.004	0.400 ± 0.010	1900 ± 100	$4E - 15 \pm 7E - 16$	2/5
	y=2.1	-	0.076 ± 0.005	0.423 ± 0.013	1988 ± 110	$3.2E - 16 \pm 5E - 17$	1/3
	y=2.3	-	0.072 ± 0.005	0.398 ± 0.013	2020 ± 110	$2E - 17 \pm 5E - 18$	1/3
	y=0.1	K^+	0.091 ± 0.005	0.250 ± 0.010	700 ± 85	$1.5E - 6 \pm 5E - 7$	6/3
	y=0.3	-	0.087 ± 0.005	0.200 ± 0.010	700 ± 62	$1.7E - 7 \pm 4E - 8$	5/5
	y=0.5	-	0.082 ± 0.005	0.280 ± 0.008	720 ± 66	$1.2E - 8 \pm 6E - 9$	7/2
	y=0.7	-	0.079 ± 0.006	0.210 ± 0.012	665 ± 88	$1.45E - 9 \pm 5E - 10$	27/6
y=0.9	-	0.076 ± 0.005	0.250 ± 0.009	665 ± 70	$1E - 10 \pm 6E - 11$	5/8	
y=1.1	-	0.074 ± 0.006	0.248 ± 0.009	600 ± 60	$6E - 12 \pm 6E - 13$	15/7	
y=1.3	-	0.069 ± 0.004	0.245 ± 0.009	600 ± 71	$5E - 13 \pm 7E - 14$	8/4	
y=1.5	-	0.066 ± 0.006	0.219 ± 0.011	635 ± 80	$3.9E - 14 \pm 7E - 15$	12/4	

Table 1. Continue.

Collisions	Rapidity	Particle	T_0 (GeV)	β_T (c)	$V(fm^3)$	N_0	χ^2/dof
Fig. 4 p-p 20 GeV	y=0.1	K^-	0.091 ± 0.006	0.260 ± 0.010	700 ± 92	$6.1E - 7 \pm 4E - 8$	10/6
	y=0.3	-	0.087 ± 0.005	0.200 ± 0.010	700 ± 62	$5.4E - 8 \pm 5E - 9$	6/5
	y=0.5	-	0.082 ± 0.005	0.280 ± 0.008	722 ± 53	$4.8E - 9 \pm 5E - 10$	3/2
	y=0.7	-	0.079 ± 0.005	0.200 ± 0.011	680 ± 70	$3.3E - 10 \pm 7E - 11$	8/2
	y=0.9	-	0.076 ± 0.004	0.250 ± 0.007	665 ± 55	$2.2E - 11 \pm 5E - 2$	5/4
	y=1.1	-	0.072 ± 0.005	0.250 ± 0.008	605 ± 50	$1.3E - 12 \pm 5E - 13$	8/2
	y=1.3	-	0.068 ± 0.005	0.245 ± 0.008	605 ± 65	$8.5E - 14 \pm 5E - 15$	2/-
	y=1.5	-	0.064 ± 0.005	0.225 ± 0.009	630 ± 70	$4.6E - 15 \pm 4E - 16$	2/-
Fig. 3 p-p 31 GeV	y=0.1	K^+	0.101 ± 0.006	0.310 ± 0.010	1004 ± 120	$1.6E - 6 \pm 6E - 7$	1.5/5
	y=0.3	-	0.097 ± 0.006	0.298 ± 0.013	1000 ± 95	$1.6E - 7 \pm 4E - 8$	1/7
	y=0.5	-	0.094 ± 0.006	0.340 ± 0.010	900 ± 70	$1.6E - 8 \pm 5E - 9$	0.2/4
	y=0.7	-	0.091 ± 0.004	0.330 ± 0.010	900 ± 90	$1.4E - 9 \pm 6E - 10$	4.5/7
	y=0.9	-	0.086 ± 0.005	0.323 ± 0.012	830 ± 110	$1.3E - 10 \pm 5E - 11$	5/7
	y=1.1	-	0.082 ± 0.004	0.310 ± 0.008	830 ± 70	$3.2E - 11 \pm 4E - 12$	15/7
	y=1.3	-	0.079 ± 0.005	0.320 ± 0.012	770 ± 85	$1.2E - 12 \pm 5E - 13$	12/7
	y=1.5	-	0.075 ± 0.006	0.330 ± 0.009	780 ± 76	$9.6E - 14 \pm 5E - 15$	9/7
	y=1.7	-	0.072 ± 0.005	0.270 ± 0.011	720 ± 50	$8E - 15 \pm 7E - 16$	9/6
	y=1.9	-	0.067 ± 0.005	0.270 ± 0.012	750 ± 78	$5E - 16 \pm 5E - 17$	4.5/5
	y=2.1	-	0.068 ± 0.006	0.230 ± 0.010	700 ± 80	$4E - 17 \pm 4E - 18$	33/4
	y=2.3	-	0.063 ± 0.004	0.200 ± 0.008	700 ± 75	$3.6E - 18 \pm 5E - 19$	1/1
Fig. 4 p-p 31 GeV	y=0.1	K^-	0.100 ± 0.004	0.310 ± 0.009	1000 ± 100	$6E - 7 \pm 4E - 8$	1.5/3
	y=0.3	-	0.096 ± 0.006	0.299 ± 0.013	1000 ± 95	$5.5E - 8 \pm 4E - 9$	5/4
	y=0.5	-	0.093 ± 0.005	0.340 ± 0.011	900 ± 70	$5E - 9 \pm 5E - 10$	0.4/2
	y=0.7	-	0.090 ± 0.006	0.260 ± 0.013	900 ± 100	$4.4E - 10 \pm 4E - 11$	2/4
	y=0.9	-	0.085 ± 0.006	0.320 ± 0.010	830 ± 110	$4E - 11 \pm 5E - 12$	4.5/4
	y=1.1	-	0.082 ± 0.006	0.310 ± 0.012	830 ± 90	$2.9E - 12 \pm 7E - 13$	6/3
	y=1.3	-	0.078 ± 0.005	0.318 ± 0.010	780 ± 80	$1.8E - 13 \pm 5E - 14$	1/3
	y=1.5	-	0.074 ± 0.005	0.330 ± 0.013	780 ± 80	$1.2E - 14 \pm 5E - 15$	0.4/1
	y=1.7	-	0.070 ± 0.004	0.210 ± 0.012	750 ± 70	$5E - 16 \pm 5E - 17$	5/-
	y=1.9	-	0.067 ± 0.006	0.270 ± 0.012	750 ± 80	$3.1E - 17 \pm 6E - 18$	0.2/-
Fig. 3 p-p 40 GeV	y=0.1	K^+	0.114 ± 0.005	0.233 ± 0.010	1345 ± 100	$1.25E - 6 \pm 5E - 7$	6/7
	y=0.3	-	0.111 ± 0.006	0.240 ± 0.010	1300 ± 80	$1.3E - 7 \pm 6E - 8$	1.5/6
	y=0.5	-	0.108 ± 0.006	0.270 ± 0.012	1200 ± 100	$1.1E - 8 \pm 4E - 9$	9/7
	y=0.7	-	0.103 ± 0.006	0.290 ± 0.010	1188 ± 100	$1E - 9 \pm 7E - 10$	3/7
	y=0.9	-	0.099 ± 0.004	0.320 ± 0.012	1260 ± 110	$9.4E - 11 \pm 4E - 12$	3/7
	y=1.1	-	0.096 ± 0.005	0.350 ± 0.010	1230 ± 100	$8.5E - 12 \pm 7E - 13$	4/7
	y=1.3	-	0.093 ± 0.005	0.330 ± 0.009	1200 ± 100	$7.5E - 13 \pm 6E - 14$	5/7
	y=1.5	-	0.089 ± 0.004	0.320 ± 0.010	1200 ± 80	$6E - 14 \pm 5E - 15$	6/7
	y=1.7	-	0.084 ± 0.004	0.208 ± 0.010	1110 ± 104	$1.6E - 14 \pm 6E - 15$	11/7
	y=1.9	-	0.080 ± 0.005	0.290 ± 0.012	1200 ± 108	$4.45E - 16 \pm 4E - 17$	19/6
Fig. 4 p-p 40 GeV	y=0.1	K^-	0.112 ± 0.004	0.240 ± 0.012	1350 ± 127	$6E - 7 \pm 4E - 8$	2/5
	y=0.3	-	0.110 ± 0.005	0.240 ± 0.010	1300 ± 87	$5.7E - 8 \pm 5E - 9$	1/4
	y=0.5	-	0.106 ± 0.005	0.260 ± 0.008	1200 ± 109	$5E - 9 \pm 7E - 10$	11/5
	y=0.7	-	0.102 ± 0.005	0.285 ± 0.009	1200 ± 110	$4E - 10 \pm 6E - 11$	3/5
	y=0.9	-	0.098 ± 0.006	0.310 ± 0.011	1260 ± 120	$3.2E - 11 \pm 6E - 12$	1/4
	y=1.1	-	0.095 ± 0.005	0.350 ± 0.009	1235 ± 100	$2.7E - 12 \pm 4E - 13$	2/4
	y=1.3	-	0.092 ± 0.005	0.280 ± 0.010	1205 ± 87	$1.6E - 13 \pm 5E - 14$	2/3
	y=1.5	-	0.088 ± 0.006	0.250 ± 0.009	1200 ± 94	$9.8E - 15 \pm 6E - 16$	2/2
	y=1.7	-	0.084 ± 0.004	0.208 ± 0.012	1100 ± 150	$7E - 16 \pm 5E - 17$	5/2
	y=1.9	-	0.080 ± 0.005	0.290 ± 0.012	1200 ± 108	$1.25E - 17 \pm 5E - 18$	2.5/-
	y=2.1	-	0.076 ± 0.005	0.200 ± 0.010	1200 ± 100	$1.7E - 18 \pm 4E - 19$	0.1/-
Fig. 3 p-p 80 GeV	y=0.1	K^+	0.121 ± 0.005	0.240 ± 0.010	1708 ± 93	$1.1E - 6 \pm 6E - 7$	1.5/5
	y=0.3	-	0.118 ± 0.006	0.240 ± 0.007	1600 ± 68	$1.2E - 7 \pm 6E - 8$	2/7
	y=0.5	-	0.114 ± 0.005	0.280 ± 0.011	1660 ± 120	$1.1E - 8 \pm 4E - 9$	1.5/7
	y=0.7	-	0.110 ± 0.005	0.320 ± 0.010	1630 ± 120	$1E - 9 \pm 6E - 10$	1.5/6
	y=0.9	-	0.107 ± 0.005	0.290 ± 0.012	1638 ± 142	$9E - 11 \pm 4E - 12$	2/5
	y=1.1	-	0.105 ± 0.006	0.300 ± 0.009	1601 ± 60	$8E - 12 \pm 6E - 13$	2/7
	y=1.3	-	0.100 ± 0.006	0.272 ± 0.008	1601 ± 90	$6E - 14 \pm 7E - 15$	8/7
	y=1.5	-	0.096 ± 0.005	0.305 ± 0.010	1578 ± 90	$5E - 15 \pm 5E - 16$	2/7
	y=1.7	-	0.093 ± 0.006	0.300 ± 0.010	1500 ± 100	$5.1E - 15 \pm 5E - 16$	4/6
	y=1.9	-	0.090 ± 0.005	0.250 ± 0.011	1520 ± 108	$3.5E - 16 \pm 6E - 17$	4/6

Table 1. Continue.

Collisions	Rapidity	Particle	T_0 (GeV)	β_T (c)	$V(fm^3)$	N_0	χ^2/dof
Fig. 4 p-p 80 GeV	y=0.1	K^-	0.121 ± 0.006	0.240 ± 0.010	1700 ± 115	$5.3E - 7 \pm 4E - 8$	1.5/5
	y=0.3	-	0.118 ± 0.006	0.240 ± 0.007	1600 ± 79	$6E - 8 \pm 4E - 9$	1/4
	y=0.5	-	0.114 ± 0.004	0.280 ± 0.011	1660 ± 123	$5.8E - 9 \pm 6E - 10$	2/4
	y=0.7	-	0.110 ± 0.005	0.314 ± 0.010	1630 ± 120	$5E - 10 \pm 5E - 11$	0.4/4
	y=0.9	-	0.107 ± 0.005	0.270 ± 0.010	1638 ± 142	$3.8E - 11 \pm 6E - 12$	2/4
	y=1.1	-	0.103 ± 0.004	0.290 ± 0.008	1621 ± 120	$2.9E - 12 \pm 5E - 13$	16/5
	y=1.3	-	0.100 ± 0.004	0.262 ± 0.012	1607 ± 95	$2.3E - 13 \pm 5E - 14$	5/5
	y=1.5	-	0.096 ± 0.005	0.300 ± 0.010	1578 ± 98	$1.7E - 14 \pm 5E - 15$	0.7/2
	y=1.7	-	0.092 ± 0.005	0.270 ± 0.010	1535 ± 110	$1.2E - 15 \pm 7E - 16$	6.5/
y=1.9	-	0.089 ± 0.004	0.250 ± 0.010	1543 ± 100	$5.6E - 17 \pm 5E - 18$	2/-	
y=2.1	-	0.085 ± 0.006	0.200 ± 0.012	1570 ± 100	$6E - 19 \pm 6E - 20$	0.2/-	
Fig. 3 p-p 158 GeV	y=0.1	K^+	0.128 ± 0.006	0.230 ± 0.008	2130 ± 120	$9E - 7 \pm 7E - 8$	2/6
	y=0.3	-	0.126 ± 0.005	0.250 ± 0.011	2117 ± 110	$9.1E - 8 \pm 7E - 9$	1/6
	y=0.5	-	0.121 ± 0.005	0.275 ± 0.012	2110 ± 110	$9.2E - 9 \pm 5E - 10$	1/6
	y=0.7	-	0.120 ± 0.005	0.295 ± 0.011	2025 ± 120	$9E - 10 \pm 6E - 11$	0.5/6
	y=0.9	-	0.116 ± 0.005	0.280 ± 0.012	2000 ± 115	$8.5E - 11 \pm 5E - 12$	1/6
	y=1.1	-	0.112 ± 0.005	0.240 ± 0.010	2070 ± 130	$7E - 12 \pm 6E - 13$	2/6
	y=1.3	-	0.107 ± 0.004	0.278 ± 0.011	2050 ± 112	$6E - 13 \pm 6E - 14$	1/5
	y=1.5	-	0.105 ± 0.004	0.248 ± 0.011	2020 ± 103	$5E - 14 \pm 7E - 15$	2/5
	y=1.7	-	0.103 ± 0.005	0.268 ± 0.010	1980 ± 120	$4.1E - 15 \pm 7E - 16$	2/5
	y=1.9	-	0.098 ± 0.006	0.217 ± 0.010	1966 ± 106	$3E - 16 \pm 4E - 17$	5.5/4
	y=2.1	-	0.097 ± 0.006	0.210 ± 0.011	1993 ± 100	$2E - 17 \pm 5E - 18$	11/5
y=2.3	-	0.094 ± 0.005	0.300 ± 0.009	1960 ± 100	$4E - 18 \pm 5E - 19$	13/3	
y=2.5	-	0.090 ± 0.004	0.230 ± 0.010	1976 ± 90	$2E - 19 \pm 4E - 20$	1.5/-	
Fig. 4 p-p 158 GeV	y=0.1	K^-	0.128 ± 0.005	0.230 ± 0.009	2130 ± 126	$6E - 7 \pm 6E - 8$	1/6
	y=0.3	-	0.125 ± 0.004	0.255 ± 0.007	2130 ± 100	$5.8E - 8 \pm 6E - 9$	0.3/5
	y=0.5	-	0.122 ± 0.006	0.275 ± 0.010	2130 ± 103	$6E - 9 \pm 6E - 9$	0.5/6
	y=0.7	-	0.118 ± 0.004	0.295 ± 0.012	2057 ± 102	$5.4E - 10 \pm 4E - 11$	1/5
	y=0.9	-	0.114 ± 0.006	0.280 ± 0.012	2000 ± 115	$4.5E - 11 \pm 7E - 12$	1/7
	y=1.1	-	0.110 ± 0.006	0.230 ± 0.008	2100 ± 117	$3.7E - 12 \pm 6E - 13$	3/7
	y=1.3	-	0.106 ± 0.006	0.270 ± 0.008	2070 ± 117	$3E - 13 \pm 5E - 14$	11/6
	y=1.5	-	0.104 ± 0.005	0.238 ± 0.008	2020 ± 105	$2.3E - 14 \pm 5E - 15$	2/6
	y=1.7	-	0.101 ± 0.004	0.268 ± 0.011	1987 ± 88	$1.7E - 15 \pm 6E - 16$	30/4
	y=1.9	-	0.097 ± 0.006	0.217 ± 0.009	1971 ± 90	$1E - 16 \pm 5E - 17$	1/3
	y=2.1	-	0.094 ± 0.005	0.210 ± 0.009	1993 ± 110	$7E - 18 \pm 5E - 19$	37/2
y=2.3	-	0.092 ± 0.005	0.290 ± 0.010	1570 ± 100	$4.1E - 19 \pm 4E - 20$	2/1	
y=2.5	-	0.089 ± 0.004	0.230 ± 0.008	1980 ± 120	$6.8E - 20 \pm 6E - 21$	4/-	
Fig. 5 p-p 31 GeV	y=0.1	\bar{p}	0.120 ± 0.006	0.089 ± 0.009	800 ± 56	$1.01E - 7 \pm 6E - 8$	8/5
	y=0.3	-	0.117 ± 0.005	0.100 ± 0.008	800 ± 70	$1.25E - 8 \pm 4E - 9$	20/5
	y=0.5	-	0.113 ± 0.004	0.060 ± 0.008	800 ± 93	$6.3E - 10 \pm 5E - 11$	10/4
	y=0.7	-	0.109 ± 0.005	0.120 ± 0.010	700 ± 68	$5.6E - 11 \pm 4E - 12$	12/3
	y=0.9	-	0.060 ± 0.007	0.120 ± 0.007	755 ± 110	$2.6E - 12 \pm 4E - 13$	8/3
Fig. 5 p-p 40 GeV	y=0.1	\bar{p}	0.129 ± 0.004	0.055 ± 0.008	1100 ± 120	$8.4E - 8 \pm 4E - 9$	3/1
	y=0.3	-	0.125 ± 0.006	0.150 ± 0.009	1000 ± 110	$9.8E - 9 \pm 6E - 10$	22/5
	y=0.5	-	0.121 ± 0.005	0.120 ± 0.009	1060 ± 88	$7.8E - 10 \pm 5E - 11$	11/3
	y=0.7	-	0.116 ± 0.004	0.140 ± 0.009	1040 ± 80	$5E - 11 \pm 5E - 12$	19/4
	y=0.9	-	0.090 ± 0.005	0.100 ± 0.008	1000 ± 80	$2.5E - 12 \pm 5E - 13$	7/4
Fig. 5 p-p 80 GeV	y=0.1	\bar{p}	0.137 ± 0.006	0.120 ± 0.007	1500 ± 160	$1.5E - 7 \pm 6E - 8$	36/7
	y=0.3	-	0.133 ± 0.005	0.120 ± 0.007	1400 ± 100	$1.5E - 8 \pm 6E - 9$	10/7
	y=0.5	-	0.124 ± 0.006	0.060 ± 0.007	1426 ± 93	$1.25E - 9 \pm 5E - 10$	5/7
	y=0.7	-	0.122 ± 0.005	0.100 ± 0.007	1450 ± 120	$1E - 10 \pm 6E - 11$	4/7
	y=0.9	-	0.110 ± 0.005	0.060 ± 0.008	1410 ± 100	$8E - 12 \pm 5E - 13$	12/6
	y=1.1	-	0.107 ± 0.005	0.120 ± 0.009	1370 ± 100	$4.8E - 13 \pm 6E - 14$	10/6
	y=1.3	-	0.102 ± 0.006	0.120 ± 0.010	1300 ± 80	$3.3E - 14 \pm 4E - 15$	14/5
y=1.5	-	0.086 ± 0.006	0.290 ± 0.011	1330 ± 110	$6E - 16 \pm 6E - 17$	277/4	
Fig. 5 p-p 158 GeV	y=0.1	\bar{p}	0.144 ± 0.005	0.060 ± 0.006	1850 ± 110	$2.3E - 7 \pm 4E - 8$	4.5/8
	y=0.3	-	0.139 ± 0.006	0.100 ± 0.007	1730 ± 120	$2.3E - 8 \pm 5E - 9$	107/8
	y=0.5	-	0.134 ± 0.005	0.100 ± 0.008	1700 ± 85	$2.2E - 9 \pm 4E - 10$	7/8
	y=0.7	-	0.130 ± 0.006	0.160 ± 0.011	1647 ± 110	$2.2E - 10 \pm 6E - 11$	3/7
	y=0.9	-	0.121 ± 0.006	0.120 ± 0.009	1670 ± 120	$1.65E - 11 \pm 6E - 12$	3/6
	y=1.1	-	0.117 ± 0.004	0.120 ± 0.007	1600 ± 120	$1.3E - 12 \pm 5E - 13$	2/5
	y=1.3	-	0.113 ± 0.005	0.150 ± 0.011	1650 ± 130	$1E - 13 \pm 6E - 14$	13/6
	y=1.5	-	0.110 ± 0.005	0.150 ± 0.012	1610 ± 100	$5.3E - 15 \pm 5E - 16$	2/3
	y=1.7	-	0.106 ± 0.004	0.150 ± 0.010	1635 ± 110	$3.3E - 16 \pm 7E - 17$	3/2
y=1.9	-	0.088 ± 0.005	0.085 ± 0.006	1630 ± 100	$1.1E - 17 \pm 6E - 18$	4/1	

measured at CERN. The collision energy and rapidity slices are presented in

legends in each panel. The spectra of K^- at 0.5 and 0.7 rapidity slices are scaled with the factor 1/8 to avoid overlapping of the experimental data and solid curve with the others. The solid curve over the experimental data shows our fitting result by the blast wave model with Boltzmann Gibbs statistics. It can be seen that the Blast wave model provides an approximately well fitting of the data at all rapidity slices.

Figure 5 is similar to fig. 4, but it shows the p_T spectra of \bar{p} in pp collisions. The symbols denote the experimental data of NA61/SHINE Collaboration measured at CERN [33]. Different panels in fig. 5 show different collision energies, and different symbols represent different rapidity slices. The solid curves are the results of our fit by Eq. (1) with fluctuations.

We used the least square method in the fit process to get the minimum χ^2 . From fig.1-fig.5, the χ^2 is large in some cases which shows that the dispersion between the curve and data is large, however the fitting is approximately acceptable, but in most cases the model results describe the experimental data well in the p_T spectra of the particles produced in different rapidity slices. Each panel in each figure is followed by the corresponding result of its data/fit in order to show the dispersion of the curve from the data. In fact, the data/fit ratio is large in some cases due to the large dispersion between the curve and data.

It should be noted that the data used in this work is from a fixed target experiment, where energies are in lab frame. Therefore we need to convert it to the center of mass energies. The corresponding 20, 31, 40, 80 and 158 GeV/c energies in the lab frame are equal to 6.3, 7.7, 8.8, 12.3 and 17.3 GeV respectively in the center of mass frame. In addition, The rapidity of the particle was measured in the cms system as $y = \text{atanh}\beta_L$, where β_L represents the longitudinal component of the velocity and is given by $\beta_L = p_L/E$ with $c = 1$, whereas E and p_L are the energy and longitudinal momentum in the cms frame.

To study the change in trend of parameters with rapidity and collision energy, Figure 6 shows the dependencies of kinetic freeze-out temperature (T_0) on rapidity and energy for the production of different particles in pp collisions. Panel (a), (b) and (c) corresponds to pion, kaon and anti-proton respectively. The closed and open symbols in panel (a)-(c) represent the positively and negatively charged particles respectively. The trend of symbols from left to right shows the dependence of kinetic freeze-out temperature (T_0) on rapidity. While the dependence of T_0 on energy is shown by the symbols from up to downward. One can see that T_0 increases

with the increases of collision energy. The reason behind this is that when the energy increases, the collision becomes more violent and transfers more energy which results in higher excitation of the system and naturally the system with high degree of excitation has high T_0 . On the other hand, the kinetic freeze-out temperature (T_0) decreases with the increase of rapidity from mid-rapidity region to forward rapidity, because when rapidity increases, the energy transfer in the system decreases due to large penetration between participant nucleons. In the meantime, due to less produced particles taking part in the scattering process, these degree of multiple scattering also decreases, the p_T decreases due to both the factors. In addition, it is observed that T_0 increases for heavier particles which shows the mass differential kinetic freeze-out scenario.

Figure 7 is similar to fig.6, but it shows the dependence of β_T on rapidity and energy. At present, we did not observe any dependence of β_T on rapidity and energy. Although there is energy dependence of β_T in literature [10, 17], but we can study it in more detail by analyzing more data for different particles in different collisions with different models. Furthermore, β_T is mass dependent and it is larger for lighter particles.

We would like to point out that QGP like properties are reported at LHC energies in pp collisions, where the values of T_0 and β_T are reported to be 163 ± 10 MeV and 0.49 ± 0.02 respectively [34]. It is also not possible to observe any such effect at the energies under consideration but the relevant parameter can still be checked for low energies to understand the nature of the collisions in the final state in comparison to high energy pp collisions. The values observed in our case are small compared to the one listed above that shows that no such effect is observed in low energy pp collisions.

Both T_0 and β_T show mass dependency, which reflects the formation time dependence. Hydrodynamically, heavier particles coming out of the system earlier in time with smaller radial flow velocities. This shows that as the mass increases, the formation time as well as β_T decreases whereas T_0 increases. Indeed, there are various hydrodynamical simulations which observe one set of parameters for all the particles (common freeze-out temperature as well as transverse flow velocity), but their explanation is different. Besides, we can get different results from different models, even from the same model we can get different results if the method is different and the limitations and conditions are different. The selection of T_0 and β_T is very technical and complex, such as in some cases, it depends on the range of p_T spectra, and it may also depend on the value of n_0 . If the value of n_0 is 1 or 2, it does not have an effect on the results of parameters but if it is taken as free param-

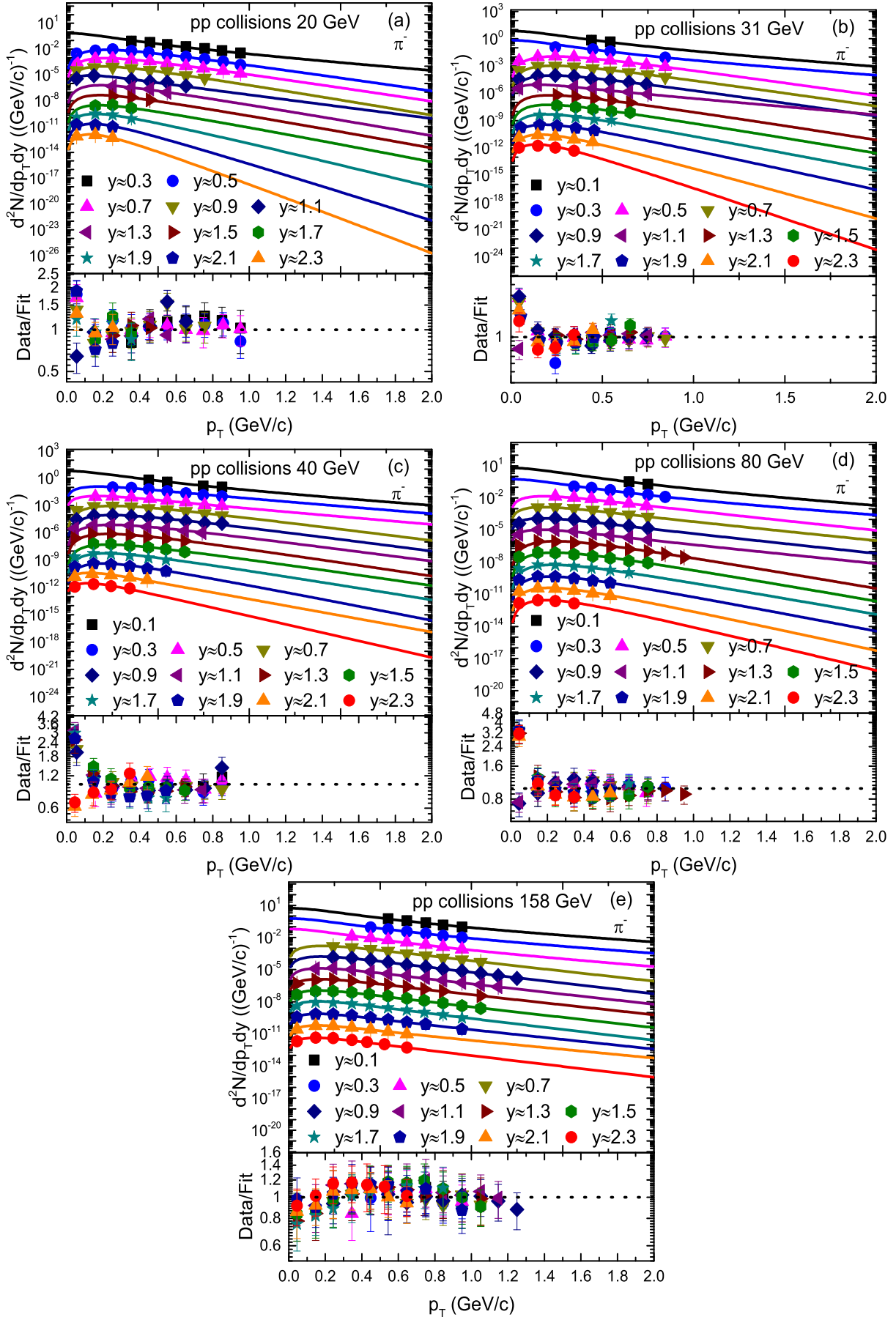


Fig. 2. Transverse momentum spectra of π^- produced in different rapidity slices in pp collisions. Panel (a)-(e) corresponds to 20, 31, 40, 80 and 158 GeV energy respectively. The symbols represent the experimental data of NA61/SHINE Collaboration measured at CERN [33]. The curves are the results of fits by the Blast Wave

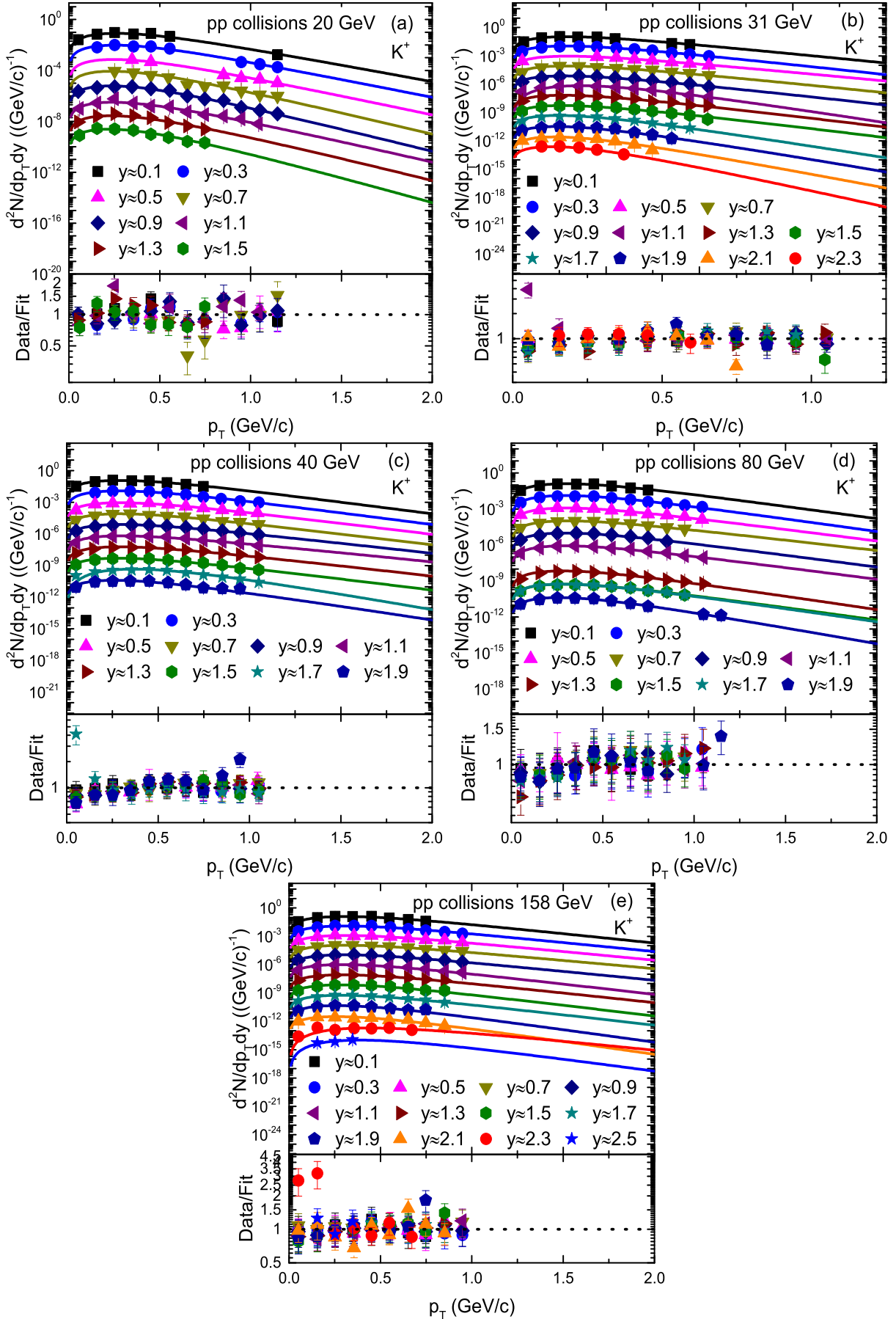


Fig. 3. Transverse momentum spectra of K^+ produced on different rapidity slices in pp collisions. Panel (a)-(e) corresponds to 20, 31, 40, 80 and 158 GeV energy respectively. The symbols represent the experimental data of NA61/SHINE Collaboration measured at CERN [33]. The curves are the results of out fits by the Blast Wave

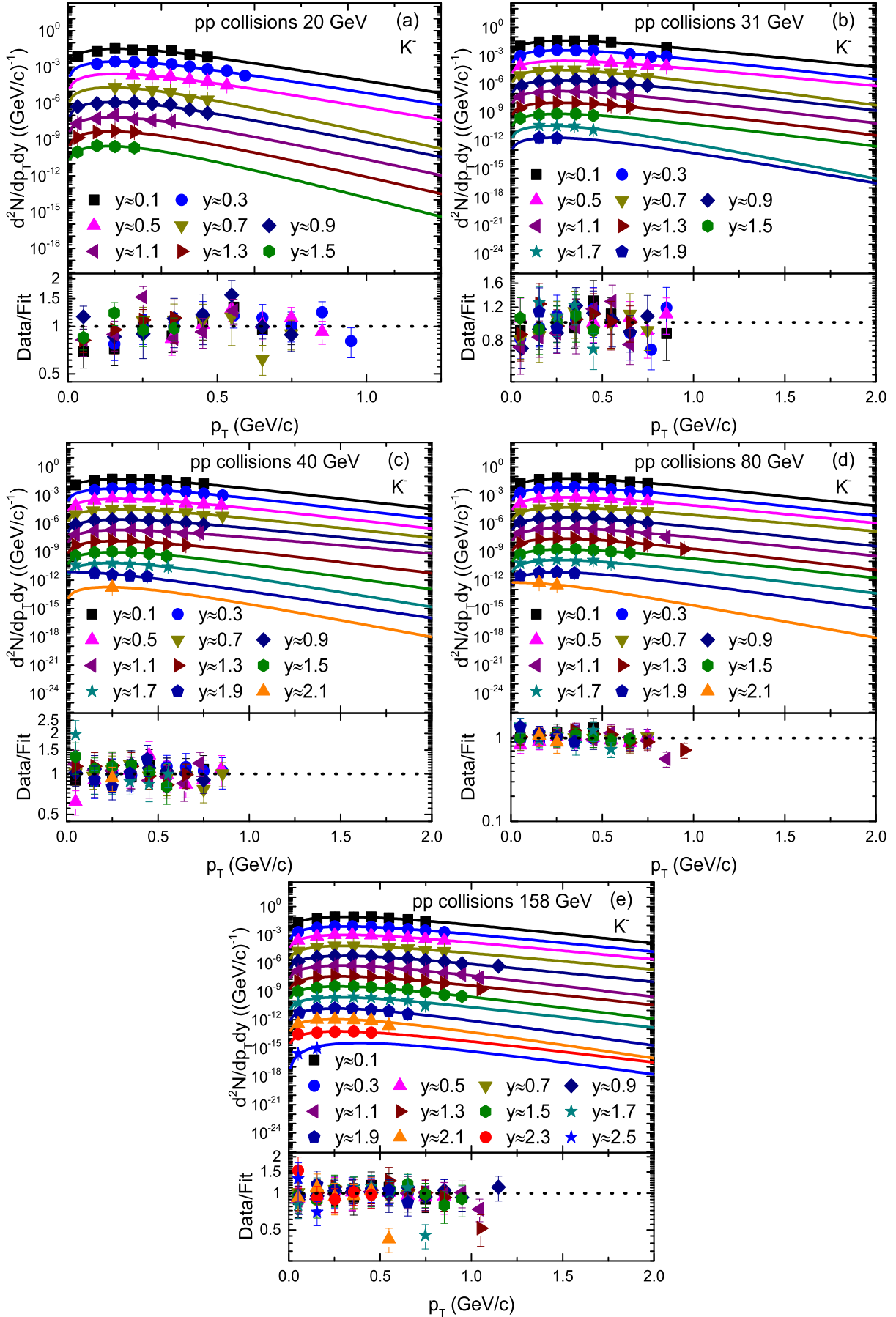


Fig. 4. Transverse momentum spectra of K^- produced in different rapidity slices in pp collisions. Panel (a)-(e) corresponds to 20, 31, 40, 80 and 158 GeV energy respectively. The symbols represent the experimental data of NA61/SHINE Collaboration measured at CERN [33]. The curves are the results of out fits by the Blast Wave

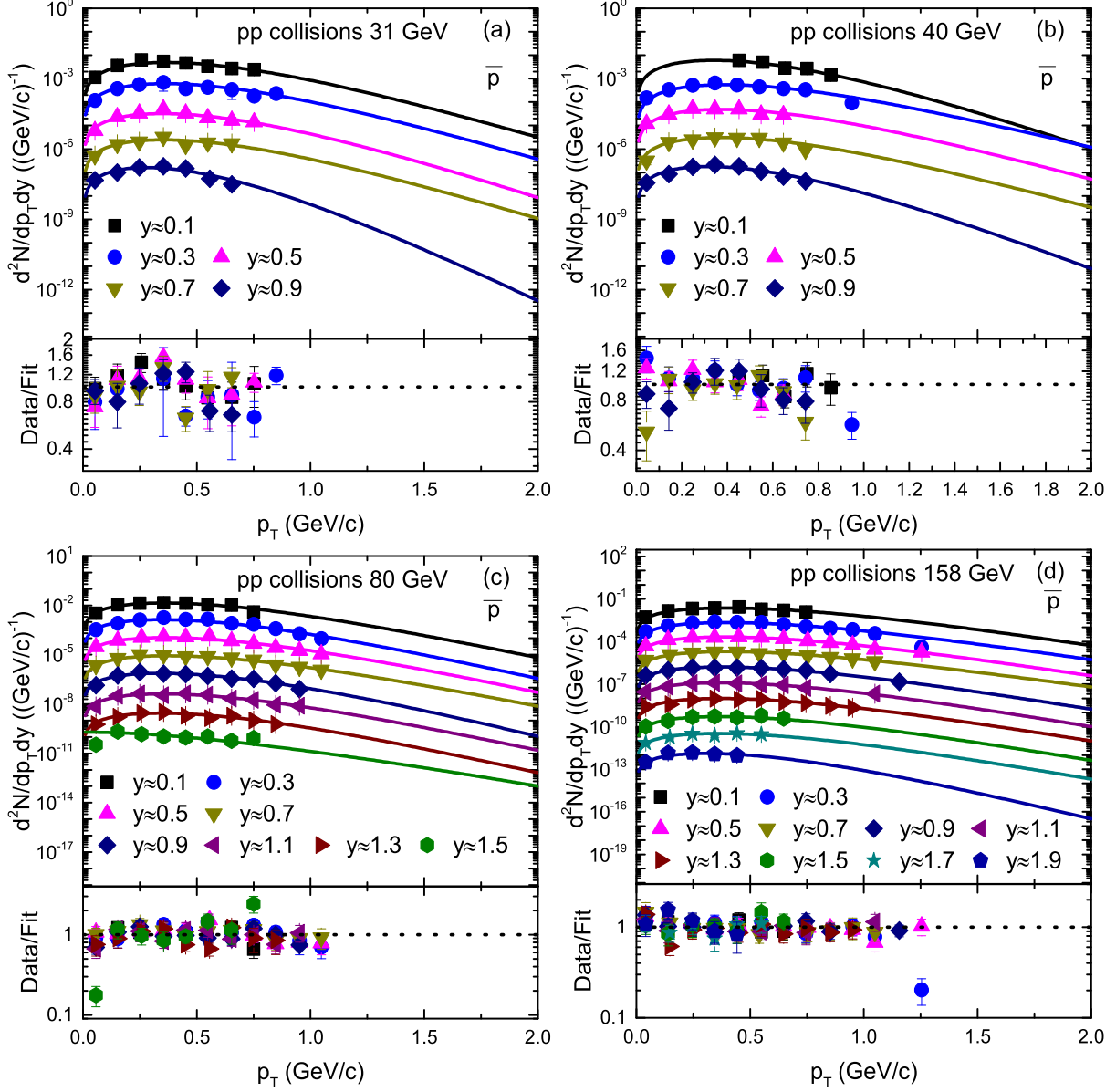


Fig. 5. Transverse momentum spectra of \bar{p} produced in different rapidity slices in pp collisions. Panel (a)-(d) corresponds to 20, 31, 40, 80 and 158 GeV energy respectively. The symbols represent the experimental data of NA61/SHINE Collaboration measured at CERN [33]. The curves are the results of out fits by the Blast Wave model with Boltzmann Gibbs statistics. The corresponding data/fit ratios are are followed in each panel.

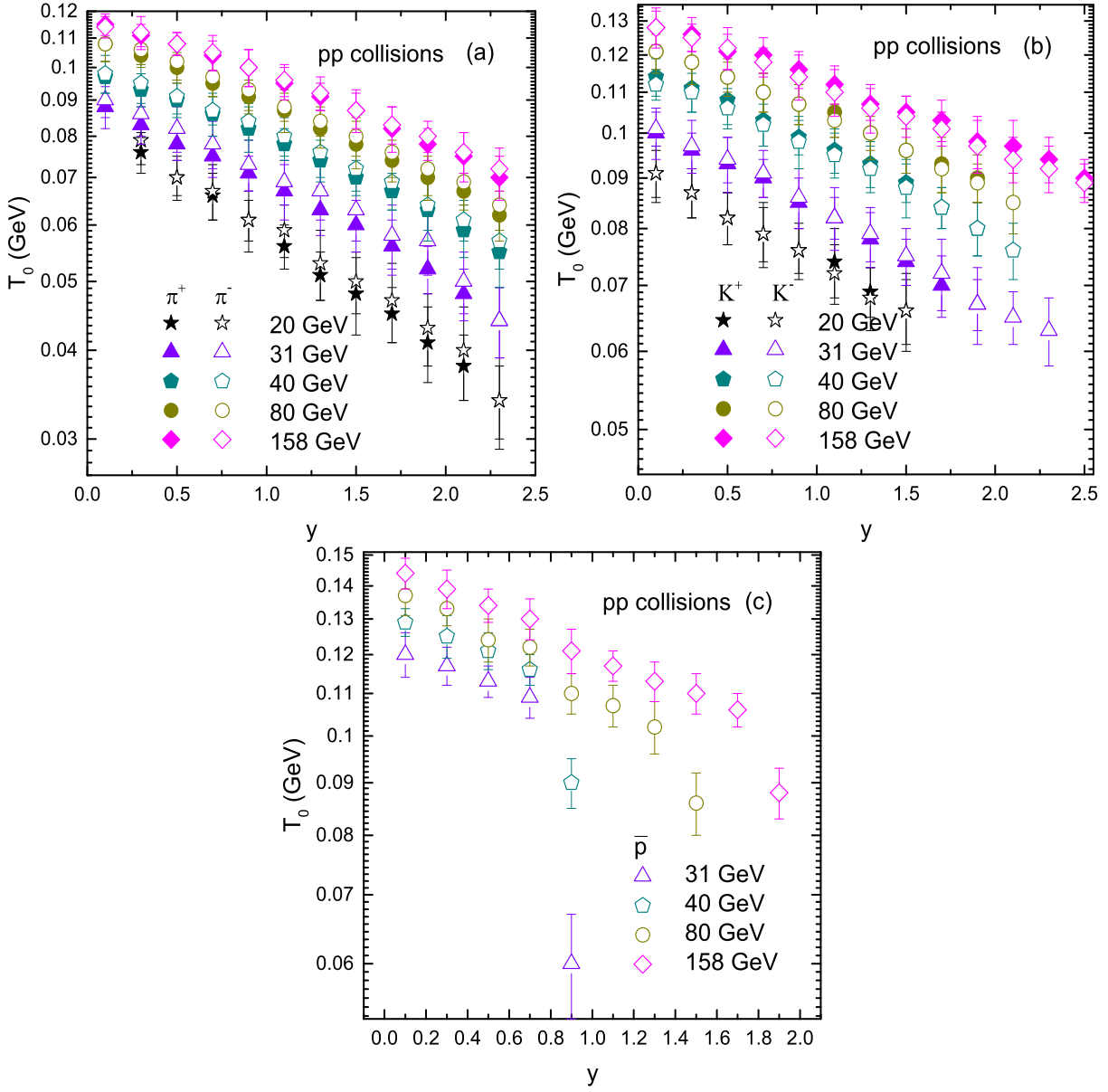


Fig. 6. Dependence of T_0 on rapidity and collision energy.

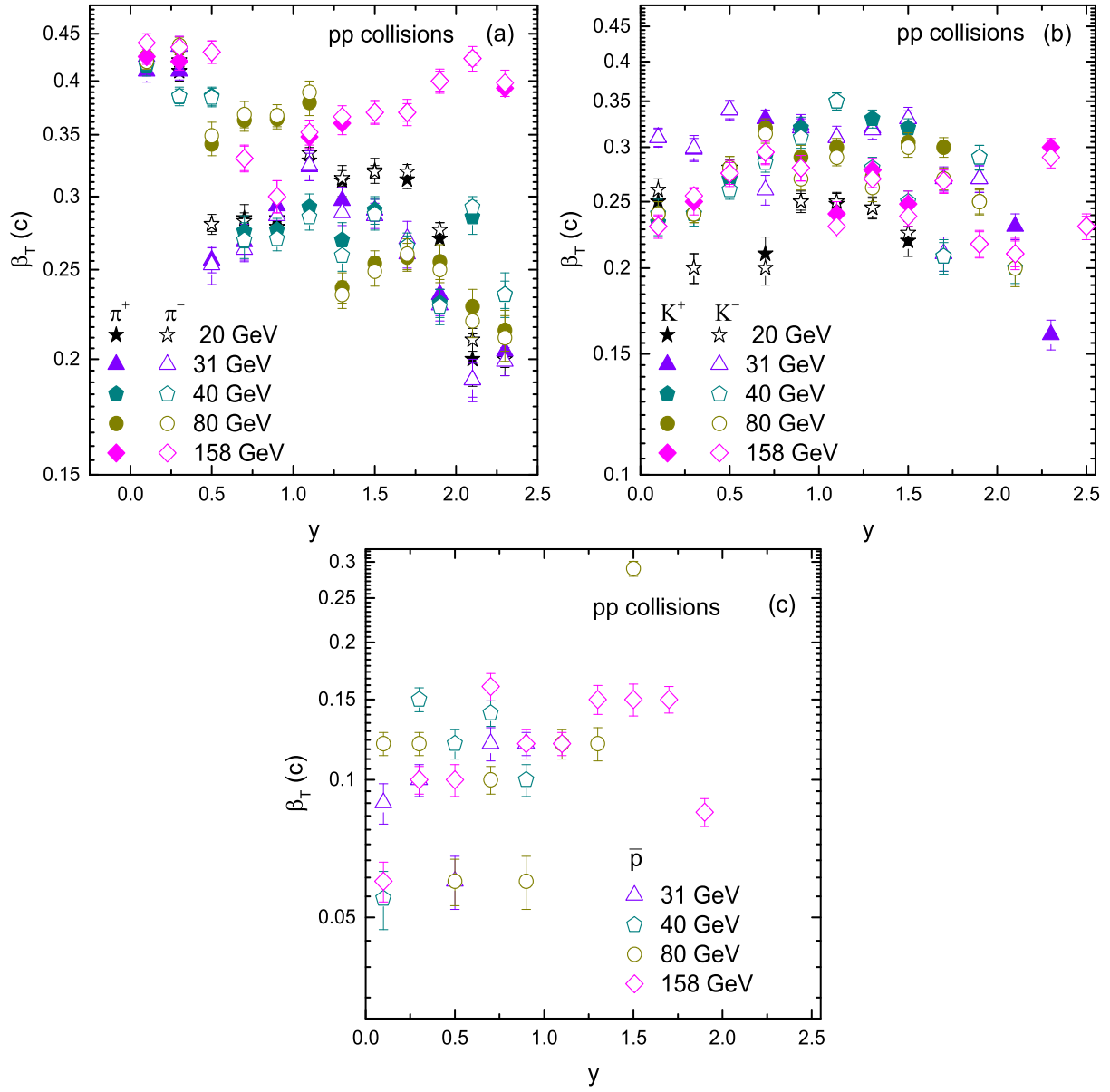


Fig. 7. Dependence of β_T on rapidity and collision energy.

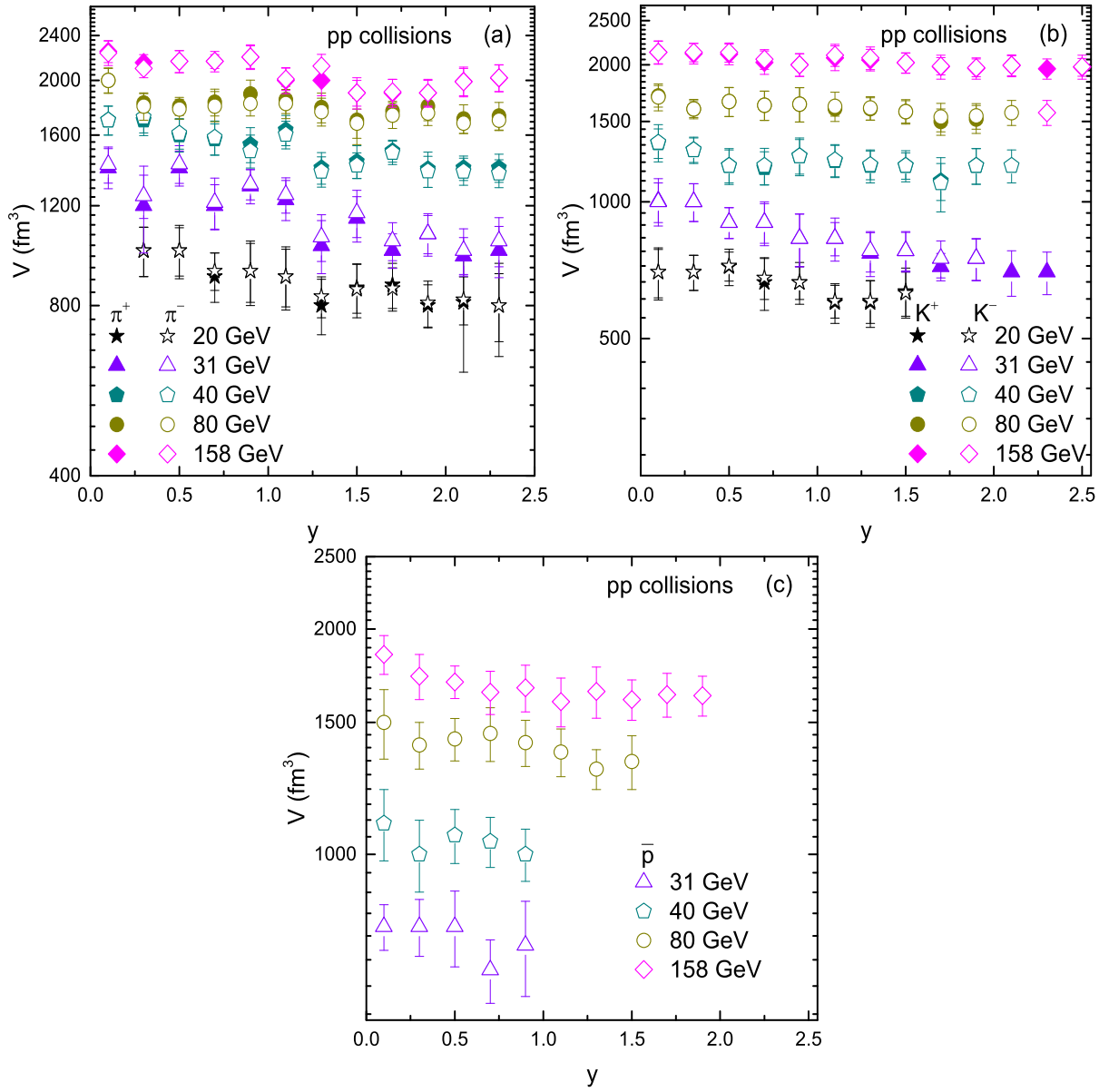


Fig. 8. Dependence of V on rapidity and collision energy.

eter, then the free parameters (especially β_T) fluctuates obviously.

Figure 8 is similar to fig. 6 and 7, but it shows the dependence of V on rapidity and energy. One can see that the kinetic freeze-out volume increases with energy. The reason behind this is that larger initial bulk system exists at high energy. The evolution time becomes longer at higher energies, and it corresponds to larger partonic system and naturally the kinetic freeze-out volume becomes larger in large partonic system. In the present work, we did not observe any clear dependence of V on rapidity because the trend of V is almost constant. However we may consider more analysis for the detailed study of dependence of V on rapidity in the future. Additionally, V is observed to be mass dependent. Larger the mass of the particle, smaller the V which shows the early freeze-out of massive particles. This result is consistent with our previous results [4, 6, 13].

4 Conclusions

We summarize here our main observations and conclusions.

(a) The transverse momentum spectra of positively and negatively charged particles produced in inelastic proton-proton collisions in different rapidity slices have been studied by the Blast Wave model with Boltzmann Gibbs statistics. The results are well in agreement with the experimental data measured by the NA61/SHINE Collaboration at CERN over an energy range from 20 GeV to 158 GeV.

(b) Kinetic freeze-out temperature increase with the increase of collision energy due to large deposition of energy in the system at higher energies, and it decreases with increase of rapidity because of less energy transfer in the system due to large penetration between participant nucleons. It is also observed that kinetic freeze-out temperature increases with mass.

(c) The transverse flow velocity is observed to have no dependence on rapidity and energy. However it is dependent on the mass of particle. Massive particles have smaller β_T .

(d) There is no dependence of kinetic freeze-out volume observed on rapidity in the present work. However, V increase with increase of energy due to longer evolution time at higher energies. It is also observed that volume differential scenario is observed as the massive particles have smaller V and they freeze-out early.

Acknowledgments This work is supported by the National Natural Science Foundation of China (Grant

Nos. 11875052, 11575190, and 11135011). We would also would like to acknowledge the support of Ajman University Internal Research Grant NO. [DGSR Ref. 2020-IRG-HBS-01].

Author Contributions All authors listed have made a substantial, direct, and intellectual contribution to the work and approved it for publication.

Data Availability Statement This manuscript has no associated data or the data will not be deposited. [Authors' comment: The data used to support the findings of this study are included within the article and are cited at relevant places within the text as references.]

Compliance with Ethical Standards

Ethical Approval The authors declare that they are in compliance with ethical standards regarding the content of this paper.

Disclosure The funding agencies have no role in the design of the study; in the collection, analysis, or interpretation of the data; in the writing of the manuscript, or in the decision to publish the results.

Conflict of Interest The authors declare that there are no conflicts of interest regarding the publication of this paper.

References

- [1] F. Becattini and U. W. Heinz, "Thermal hadron production in p p and p anti-p collisions," *Z. Phys. C* **76**, 269-286 (1997) [erratum: *Z. Phys. C* **76**, 578 (1997)] doi:10.1007/s002880050551
- [2] L. L. Li, F. H. Liu, M. Waqas, R. Al-Yusufi and A. Mujear, "Excitation functions of related parameters from transverse momentum (mass) spectra in high energy collisions," *Adv. High Energy Phys.* **2020**, 5356705 (2020) doi:10.1155/2020/5356705 [arXiv:1911.07419 [hep-ph]].
- [3] L. L. Li and F. H. Liu, "Kinetic Freeze-Out Properties from Transverse Momentum Spectra of Pions in High Energy Proton-Proton Collisions," *MDPI Physics* **2**, no.2, 277-308 (2020) doi:10.3390/physics2020015 [arXiv:1805.03342 [hep-ph]].
- [4] M. Waqas, F. H. Liu, L. L. Li and H. M. Alfanda, "Effective (kinetic freeze-out) temperature, transverse flow velocity and kinetic freeze-out volume in high energy collisions," *Nucl. Sci. Tech.* **31**, no.11, 109 (2020) doi:10.1007/s41365-020-00821-7 [arXiv:2001.06796 [hep-ph]].

- [5] M. Waqas and F. H. Liu, “Initial, effective, and kinetic freeze-out temperatures from transverse momentum spectra in high-energy proton(deuteron)–nucleus and nucleus–nucleus collisions,” *Eur. Phys. J. Plus* **135**, no.2, 147 (2020) doi:10.1140/epjp/s13360-020-00213-1 [arXiv:1911.01709 [hep-ph]].
- [6] M. Waqas, F. H. Liu and Z. Wazir, “Dependence of temperatures and kinetic freeze-out volume on centrality in Au-Au and Pb-Pb collisions at high energy,” *Adv. High Energy Phys.* **2020**, 8198126 (2020) doi:10.1155/2020/8198126 [arXiv:2004.03773 [hep-ph]].
- [7] M. Waqas, G. X. Peng and Z. Wazir, “Decoupling of non-strange, strange and multi-strange particles from the system in Cu-Cu, Au-Au and Pb-Pb collisions at high energies,” [arXiv:2107.07840 [hep-ph]].
- [8] A. Puglisi, A. Sarracino, A. Vulpiani, *Phys. Rep.* **709**, 1 (2017).
- [9] Waqas. M, Liu. F-H, Fakhraddin. S and Rahim. M.A, Possible scenarios for single, double, or multiple kinetic freeze-out in high energy collisions, *Indian J. Phys.* **2019**, *93*, 1329-1343 doi:10.1007/s12648-019- 01396-9 [arXiv:1806.04312 [nucl-th]].
- [10] Waqas. M, and Li. B. C Kinetic freeze-out temperature and transverse flow velocity in Au-Au collisions at RHIC-BES energies, *Adv. High Energy Phys.* **2020**, *2020*, 1787183. [arXiv:1909.11339 [hep-ph]].
- [11] Thakur. D, Tripathy. S, Garg. P, Sahoo. R and Cleymans. J, Indication of Differential Kinetic Freeze-out at RHIC and LHC Energies, *Acta Phys. Polon. Supp.* **2016**, *9*, 329 doi:10.5506/APhysPolBSupp.9.329 [arXiv:1603.04971 [hep-ph]]
- [12] Khuntia. A, Sharma. H, Kumar Tiwari. S, Sahoo. R and Cleymans. J, Radial flow and differential freeze-out in proton-proton collisions at 7 TeV at the LHC, *Eur. Phys. J. A* **2019**, *55*, 3 doi:10.1140/epja/i2019-12669-6 [arXiv:1808.02383 [hep-ph]].
- [13] Waqas. M, Peng. G. X and Liu. F-H. An evidence of triple kinetic freezeout scenario observed in all centrality intervals in Cu-Cu, Au-Au and PbPb collisions at high energies, *J. Phys. G* **48**, no.7, 075108 (2021) doi:10.1088/1361-6471 [arXiv:2101.07971 [hep-ph]].
- [14] Shao. M, Yi. L, Tang. Z, Chen. H, Li. C and Xu. Z, Examine the species and beam-energy dependence of particle spectra using Tsallis Statistics, *J. Phys. G* **2010**, *37*, 085104 doi:10.1088/0954-3899/37/8/085104 [arXiv:0912.0993 [nucl-ex]].
- [15] H. L. Lao, F. H. Liu, B. C. Li and M. Y. Duan, “Kinetic freeze-out temperatures in central and peripheral collisions: Which one is larger?,” *Nucl. Sci. Tech.* **29**, no.6, 82 (2018) doi:10.1007/s41365-018-0425-x [arXiv:1703.04944 [nucl-th]].
- [16] M. Waqas and G. X. Peng, “Study of Proton, Deuteron, and Triton at 54.4 GeV,” *Adv. High Energy Phys.* **2021**, 6674470 (2021) doi:10.1155/2021/6674470 [arXiv:2103.07852 [hep-ph]].
- [17] Kumar. L, et al. (STAR Collaboration), Systematics of kinetic freeze-out properties in high energy collisions from STAR, *Nucl. Phys. A* **931**, 1114 (2014).
- [18] M. Waqas, F. H. Liu, R. Q. Wang and I. Siddique, “Energy scan/dependence of kinetic freeze-out scenarios of multi-strange and other identified particles in central nucleus-nucleus collisions,” *Eur. Phys. J. A* **56**, no.7, 188 (2020) doi:10.1140/epja/s10050-020-00192-y [arXiv:2007.00825 [hep-ph]].
- [19] M. Waqas, G. X. Peng, F. H. Liu and Z. Wazir, “Effects of coalescence and isospin symmetry on the freezeout of light nuclei and their anti-particles,” [arXiv:2105.01300 [hep-ph]].
- [20] Schnedermann. E, Sollfrank. J and Heinz. U. W, Thermal phenomenology of hadrons from 200-A/GeV S+S collisions, *Phys. Rev. C* **48**, 2462-2475 (1993). doi:10.1103/PhysRevC.48.2462 [arXiv:nucl-th/9307020 [nucl-th]]
- [21] B. I. Abelev *et al.* [STAR], “Systematic Measurements of Identified Particle Spectra in pp, d^+ Au and Au+Au Collisions from STAR,” *Phys. Rev. C* **79**, 034909 (2009) doi:10.1103/PhysRevC.79.034909 [arXiv:0808.2041 [nucl-ex]].
- [22] O. Ristea, A. Jipa, C. Ristea, T. Esanu, M. Calin, A. Barzu, A. Surtu and I. Abu-Quoad, “Study of the freeze-out process in heavy ion collisions at relativistic energies,” *J. Phys. Conf. Ser.* **420**, 012041 (2013) doi:10.1088/1742-6596/420/1/012041
- [23] Z. Tang, Y. Xu, L. Ruan, G. van Buren, F. Wang and Z. Xu, “Spectra and radial flow at RHIC with Tsallis statistics in a Blast-Wave description,” *Phys. Rev. C* **79**, 051901 (2009) doi:10.1103/PhysRevC.79.051901 [arXiv:0812.1609 [nucl-ex]].
- [24] S. Takeuchi, K. Murase, T. Hirano, P. Huovinen and Y. Nara, “Effects of hadronic rescattering on multistrange hadrons in high-energy nuclear collisions,” *Phys. Rev. C* **92**, no.4, 044907 (2015) doi:10.1103/PhysRevC.92.044907 [arXiv:1505.05961 [nucl-th]].
- [25] B. I. Abelev *et al.* [STAR], “Identified particle production, azimuthal anisotropy, and interferometry measurements in Au+Au collisions at $s(\text{NN})^{1/2} = 9.2$ - GeV,” *Phys. Rev. C* **81**, 024911 (2010) doi:10.1103/PhysRevC.81.024911 [arXiv:0909.4131 [nucl-ex]].
- [26] U. W. Heinz, “Concepts of heavy ion physics,” [arXiv:hep-ph/0407360 [hep-ph]].
- [27] H. Heiselberg and A. M. Levy, “Elliptic flow and HBT in noncentral nuclear collisions,” *Phys. Rev. C* **59**, 2716-2727 (1999) doi:10.1103/PhysRevC.59.2716 [arXiv:nucl-th/9812034 [nucl-th]].
- [28] H. R. Wei, F. H. Liu and R. A. Lacey, “Kinetic freeze-out temperature and flow velocity extracted from transverse momentum spectra of final-state light flavor particles produced in collisions at RHIC and LHC,” *Eur. Phys. J. A* **52**, no.4, 102 (2016) doi:10.1140/epja/i2016-16102-6 [arXiv:1601.07045 [hep-ph]].
- [29] H. L. Lao, H. R. Wei, F. H. Liu and R. A. Lacey, “An evidence of mass-dependent differential kinetic freeze-out scenario observed in Pb-Pb collisions at 2.76 TeV,” *Eur.*

- Phys. J. A **52**, no.7, 203 (2016) doi:10.1140/epja/i2016-16203-2 [arXiv:1601.00045 [nucl-th]]
- [30] J. Cleymans and D. Worku, “Relativistic Thermodynamics: Transverse Momentum Distributions in High-Energy Physics,” Eur. Phys. J. A **48**, 160 (2012) doi:10.1140/epja/i2012-12160-0 [arXiv:1203.4343 [hep-ph]].
- [31] H. R. Wei, F. H. Liu and R. A. Lacey, “Disentangling random thermal motion of particles and collective expansion of source from transverse momentum spectra in high energy collisions,” J. Phys. G **43**, no.12, 125102 (2016) doi:10.1088/0954-3899/43/12/125102 [arXiv:1509.09083 [nucl-ex]].
- [32] A. Aduszkiewicz *et al.* [NA61/SHINE], “Measurements of π^\pm , K^\pm , p and \bar{p} spectra in proton-proton interactions at 20, 31, 40, 80 and 158 GeV/c with the NA61/SHINE spectrometer at the CERN SPS,” Eur. Phys. J. C **77**, no.10, 671 (2017) doi:10.1140/epjc/s10052-017-5260-4 [arXiv:1705.02467 [nucl-ex]].
- [33] J. Adam *et al.* [ALICE], Nature Phys. **13**, 535-539 (2017) doi:10.1038/nphys4111 [arXiv:1606.07424 [nucl-ex]].